⌘ *Author's Choice*

THE JOURNAL OF BIOLOGICAL CHEMISTRY VOL. 287, NO. 11, pp. 8424–8433, March 9, 2012
Published in the U.S.A.

Biochemical Inhibition of the Acetyltransferases ATase1 and ATase2 Reduces β-Secretase (BACE1) Levels and Aβ Generation*[S]

Received for publication, October 6, 2011, and in revised form, January 18, 2012 Published, JBC Papers in Press, January 20, 2012, DOI 10.1074/jbc.M111.310136

Yun Ding[‡§1], Mi Hee Ko[‡1,2], Mariana Pehar[‡], Frank Kotch[¶3], Noel R. Peters[¶], Yun Luo[¶], Shahriar M. Salamat[‖], and Luigi Puglielli[‡§4]**

*From the [‡]Department of Medicine, the [§]Neuroscience Training Program, the [¶]Small Molecule Screening Facility, and the [‖]Department of Pathology, University of Wisconsin-Madison, Madison, Wisconsin 53705 and the **Geriatric Research Education Clinical Center, VA Medical Center, Madison, Wisconsin 53705*

Background: The acetyltransferases ATase1 and ATase2 regulate the levels of BACE1, which is involved in the pathogenesis of Alzheimer disease (AD).
Results: Both ATases are up-regulated in the brain of AD patients. ATase1/ATase2 inhibitors were identified. Structure-activity relationship, mechanisms of action, and biological effects were determined.
Conclusion: ATase1/ATase2 inhibitors down-regulate levels and activity of BACE1.
Significance: ATase1/ATase2 are potential targets to prevent AD.

The cellular levels of β-site APP cleaving enzyme 1 (BACE1), the rate-limiting enzyme for the generation of the Alzheimer disease (AD) amyloid β-peptide (Aβ), are tightly regulated by two ER-based acetyl-CoA:lysine acetyltransferases, ATase1 and ATase2. Here we report that both acetyltransferases are expressed in neurons and glial cells, and are up-regulated in the brain of AD patients. We also report the identification of first and second generation compounds that inhibit ATase1/ATase2 and down-regulate the expression levels as well as activity of BACE1. The mechanism of action involves competitive and non-competitive inhibition as well as generation of unstable intermediates of the ATases that undergo degradation.

The membrane protein β-site APP-cleaving enzyme 1 (BACE1)[5] is responsible for the β cleavage of the amyloid precursor protein (APP). The cleavage, which has been linked to the pathogenesis of Alzheimer disease (AD), results in the generation of a small APP fragment (commonly referred to as C99) acting as the immediate substrate for γ secretase (1). The sequential β/γ processing of APP results into two small fragments, the amyloid β-peptide (Aβ), and the APP intracellular domain (AICD). Both have neurotoxic properties and both have been linked to the pathogenesis of AD (2–9). Importantly, BACE1 acts as the rate-limiting enzyme. As a result, genetic disruption of BACE1 in the mouse abolishes both β and γ cleavage of APP and prevents AD neuropathology (10, 11). Therefore, mechanisms that regulate levels and/or activity of BACE1 could serve for therapeutic purposes. Unfortunately, biochemical design of BACE1 inhibitors has proven to be challenging due to the rather large size of the catalytic pocket of the enzyme (12). Therefore, approaches that affect expression levels rather than catalytic activity of BACE1 are being actively sought.

We recently reported that nascent BACE1 is transiently acetylated in the lumen of the endoplasmic reticulum (ER) (13) by two ER-based acetyl-CoA:lysine acetyltransferases, which we named ATase1 (also known as camello-like 2 and *N*-acetyltransferase 8B) and ATase2 (also known as camello-like 1 and *N*-acetyltransferase 8) (14). The N^{ϵ}-lysine acetylation regulates the ability of nascent BACE1 to complete maturation. In fact, the acetylated intermediates of the nascent protein are able to reach the Golgi apparatus and complete maturation while the non-acetylated intermediates are retained and degraded in the ER Golgi intermediate compartment (ERGIC) (13, 15). *Ex vivo* studies show that the levels of BACE1 are tightly regulated by the ATases. Specifically, up-regulation of ATase1 and ATase2 increases the levels of BACE1 and the generation of Aβ while siRNA-mediated down-regulation of either transferase achieves the opposite effects (14).

Here, we report that both acetyltransferases are expressed in neurons and glial cells, and are up-regulated in the brain of AD patients. We also report the identification of novel biochemical inhibitors of ATase1 and ATase2 that significantly reduce the

* This research was supported, in whole or in part, by National Institutes of Health (NIH)/NIA Grants AG028569 and AG033514, Department of Veterans Affairs, Rotary Coins for Alzheimer Research Trust Fund, and UW Institute for Clinical and Translational Research (funded through an NCRR/NIH Clinical and Translational Science Award, 1UL1RR025011).
⌘ *Author's Choice*—Final version full access.
[S] This article contains supplemental Tables SI–SIII, Figs. S1–S8, and experimental methods.
[1] Both authors contributed equally to this work.
[2] Present address: Korea National Institute of Health, Chungcheongbuk-do, South Korea.
[3] Present address: Pfizer Worldwide Research and Development, Pearl River, NY.
[4] To whom correspondence should be addressed: Department of Medicine, University of Wisconsin-Madison, VAH-GRECC, 2500 Overlook Terrace, Madison, WI 53705. Tel.: 608-256-1901 (ext. 11569); Fax: 608-280-7291; E-mail: lp1@medicine.wisc.edu.
[5] The abbreviations used are: BACE1, β-site APP-cleaving enzyme 1; αsAPP, α-secreted APP; Aβ, amyloid β-peptide; AD, Alzheimer disease; AICD, APP intracellular domain; APP, amyloid precursor protein; ATase, acetyl-CoA lysine acetyltransferase; βsAPP, β-secreted APP; ER, endoplasmic reticulum; ERGIC, ER Golgi intermediate compartment.

levels of BACE1 and the generation of Aβ in cellular systems. The biochemical properties of first and second generation compounds as well as mechanisms of inhibition are also described.

EXPERIMENTAL PROCEDURES

The complete description of the compounds used in this study can be found under supplemental experimental materials.

Antibodies—The following antibodies were used in this study: anti-acetylated lysine (ab409; Abcam); anti-BACE1 (ab2077; Abcam); anti-Myc (sc-40; Santa Cruz Biotechnology); anti-ATases/NAT8 (AP4957c; Abgent); anti-actin (A1978; Sigma); anti-C99 (M066-3; MBL); anti-acetylated H3 (06-599, Millipore); anti-acetylated H4 (06-866, Millipore); anti-αPCNA (AP2835b, Abgent).

Western Blot Analysis—Western blotting was performed on a 4–12% Bis-Tris SDS-PAGE system (NuPAGE; Invitrogen) as described previously (14–19). Samples were imaged with classical chemiluminescence or with the LiCor Odyssey Infrared Imaging System (LI-COR Biosciences). For chemiluminescent detection, HRP-conjugated anti-mouse or anti-rabbit secondary antibodies were used at 1:6000 dilution in 3% BSA/TBST (GE Healthcare). Detection was performed with either Lumiglo (KPL) or ECL Plus (GE Healthcare). For infrared imaging, goat anti-rabbit Alexa Fluor 680- or anti-mouse Alexa Fluor 800-conjugated secondary antibodies were used. For quantification, values were normalized to the appropriate loading control (shown in the figures).

Cell Cultures and Animals—Immortalized cell lines (CHO, H4, SH-SY5Y, SHEP, PC-12) were grown in DMEM (Invitrogen) supplemented with 10% fetal bovine serum (FBS) and penicillin/streptomycin (Mediatech) as described before (13, 14, 16). Mouse primary neurons were prepared as described (16) and plated on poly-(L-lysine)-coated 6-well plates (Becton Dickinson Labware) for 2 h. Neurons were then changed to Neurobasal medium containing 2% B27 supplement (Invitrogen) in the absence of serum or antibiotics. Cultures grown in serum-free media yielded 99.5% neurons and 0.5% glia. Microscopically, glial cells were not apparent in cultures at the time they were used for experimental analysis.

Non-transgenic C57B6/6J and $p44^{+/+}$ transgenic mice were euthanized according to the NIH Guide for the Care and Use of Laboratory Animals. For Western blot analysis, brains were immediately removed for the isolation of neocortex and hippocampus. Tissue was processed for protein extraction in GTIP buffer (100 mM Tris, pH 7.6, 20 mM EDTA, 1.5 M NaCl) supplemented with 1% Triton X-100 (Roche), 0.25% Nonidet P-40 (Roche), and a complete protease inhibitors mixture (Roche), as described before (15, 16, 19). For histology and immunostaining, brains were immediately processed as described below.

All animal experiments were carried out in accordance with the NIH Guide for the Care and Use of Laboratory Animals and were approved by the Institutional Animal Care and Use Committee of the University of Wisconsin-Madison.

Human Brain Tissue—Brain tissue from late-onset AD patients and age-matched controls was kindly provided by the Brain Bank of the Neuropathology Core of the Wisconsin Alzheimer Disease Research Center (established by grant P50-AG033514 from NIH/NIA). The use of human brain tissue was approved by the University of Wisconsin-Madison Institutional Review Board in accordance with US federal regulations (as defined under 45 CFR 46.102(f)). Pathological grading of AD patients is found in supplemental Table SI.

Histology and Immunostaining—Mouse brains were removed, fixed overnight in 10% neutral buffered formalin, and paraffin-embedded using standard techniques. Coronal tissue sections (5 μm) were prepared using a microtome. Paraffin-embedded tissue sections from AD patients and age-matched controls were obtained from the Wisconsin Alzheimer Disease Research Center, as described above. Following standard deparaffinization and rehydration, the tissue sections were processed for immunofluorescence. Antigen retrieval was performed in 100 mM citrate buffer (pH 6) heated in an autoclave. After washing with PBS, tissue sections were permeabilized with 0.1% Triton X-100 in PBS and blocked for 2 h with 10% goat serum, 2% bovine serum albumin, and 0.1% Triton X-100 in PBS. Sections were then incubated with primary antibodies (diluted in blocking solution) overnight at 4°C. The following primary antibodies were used: mouse anti-NeuN (clone A60; 1:100; Chemicon-Millipore) and rabbit anti-ATases/NAT8 (1:50; Abgent). After washing with PBS, they received Alexa 594-goat anti-mouse (5 μg/ml; Molecular Probes-Invitrogen) and biotin-conjugated goat anti-rabbit (5 μg/ml; Molecular Probes-Invitrogen) for 1 h at room temperature; followed by Alexa 488-conjugated streptavidin (5 μg/ml; Molecular Probes-Invitrogen) for 1 h at room temperature. Controls were performed by omitting the primary antibody. Nuclei were counterstained with 4′,6-diamidino-2-phenylindole (DAPI; Molecular Probes-Invitrogen, Carlsbad, CA). Slides were mounted using Gel/Mount aqueous mounting medium (Electron Microscopy Sciences, Hatfield, PA) and imaged on a Zeiss Axiovert 200 inverted fluorescent microscope.

Preparation of Cytosolic and Nuclear Fractions—Cytosolic and nuclear extracts were prepared as described before (17). For cytosolic extracts, cells were homogenized in homogenization buffer containing 25 mM Tris-HCl, pH 7.4, 0.5 mM EDTA, 0.5 mM EGTA, and a protease inhibitor mixture. The homogenates were centrifuged at 14,000 × *g* for 15 min, and supernatants were collected as cytosolic proteins.

For nuclear extracts cells were scraped into ice-cold phosphate-buffered saline and collected by centrifugation. The cell pellets were suspended in 3 volumes of lysis buffer (20 mM Hepes, pH 7.9, 10 mM KCl, 1 mM EDTA, pH 8.0, 0.2% Nonidet P-40, 10% glycerol, and a protease inhibitor mixture) followed by incubation on ice for 10 min. Cell suspensions were gently pipetted up and down; the lysates were then centrifuged at 14,000 × *g* for 5 min at 4 °C to obtain nuclear pellets. Nuclear pellets were washed twice with cell lysis buffer (lacking Nonidet P-40 and protease inhibitor mixture) and then resuspended in 2 volumes of nuclear extract buffer (20 mM Hepes, pH 7.9, 10 mM KCl, 1 mM EDTA, pH 8.0, 420 mM NaCl, 20% glycerol, and a protease inhibitor mixture). The nuclei were extracted by incubation at 4 °C for 30 min with gentle agitation followed by centrifugation at 14,000 × *g* at 4 °C for 5 min; the resultant supernatant fraction was used as a nuclear extract.

AcetylCoA:Lysine Acetyltransferase Assay—The acetyl:CoA lysine acetyltransferase activity of ATase1 and ATase2 was assayed as described before (14). Briefly, we adapted a commercially available fluorescent kit (cat. no. 10006515, Cayman Chemicals) as following: as source of the enzymatic activity, we used affinity purified ATase1-myc and ATase2-myc at the final concentration of 300 ng/μl; as donor of the acetyl group, we used acetyl-CoA at the final concentration of 12.5 μM. ATase1 and ATase2 were purified with the ProFound c-myc-Tag IP/Co-IP kit (Pierce) as suggested by the manufacturer and already described in our previous work (14). The acetyltransferase assay was performed as recommended by the manufacturer.

For kinetic analysis of ATase1 and ATase2 inhibition, the assays were performed in the presence of the indicated concentrations of compound 9, 19, and 9.I. The concentration of acetyl-CoA was varied from 0.5 to 15 μM. Values were plotted as a Lineweaver-Burk plot using Graphpad Prism software.

Real Time PCR—Real-time PCR was carried out as described before (14). The cycling parameters were: 95 °C, 10 s; 55 °C, 60 °C, or 61 °C, 10 s; 72 °C, 15 s, for a maximum of 40 cycles. Controls without reverse transcription were included in each assay. PCR primers specific to each gene were: ATase1/NAT8B-human, 5′-AGACGGGCCAGTCCTTCTTC-3′ and 5′-GCACAGAAAGGTCATTGCAGTCAG-3′; ATase2/NAT8-human, 5′-TCCTTGCCAAAAAACCCTGG-3′ and 5′-ATGCCCACCACCTTCTCTTCA-3′; glyceraldehyde-3-phosphate dehydrogenase (GAPDH)-human, 5′-TTTGTCAAGCTCATTTCCTGGTA-3′ and 5′-TTCAAGGGGTCTACATGGCAACTG-3′. ATase1 and ATase2 expression levels were normalized against GAPDH levels and are expressed as percent of control.

Aβ Determination—For Aβ determinations in the conditioned media, H4 cells were plated in 6-well Petri dishes. When 80–90% confluent, cells were washed in PBS and incubated in 1 ml of fresh medium for 48 h in the presence or absence of inhibitors. Secreted Aβ was determined by standard sandwich ELISA as described before (13–16, 18, 19). For each sample, the levels of Aβ40, Aβ42, and Aβtotal were quantified as triplicate based upon standard curves run (on every ELISA plate) and then expressed as pmol Aβ/mg of protein. Aβ42 was constantly found to be 20–25% of total Aβ values.

Circular Dichroism—The experiments with circular dichroism (CD) were carried out at the Biophysics Instrumentation Facility (Department of Biochemistry, University of Wisconsin-Madison), which was established by funding from NSF (BIR-9512577), NIH (S10 RR13790) and the University of Wisconsin. Briefly, ATase1 and ATase2 were purified as for the acetyl:CoA lysine acetyltransferase assay and then incubated with 10 μM compound 9 or 19. The difference in the absorbances of left- and right-handed circularly polarized light impinging on the solution was measured with a 202SF CD Spectrophotometer (Aviv Biomedical) in PBS and at room temperature. Appropriate controls included PBS alone and compound 9 or 19 in the absence of the ATases.

Statistical Analysis—Data were analyzed by ANOVA and Student's *t* test comparison, using GraphPad InStat3 software. Statistical significance was reached at $p \leq 0.05$.

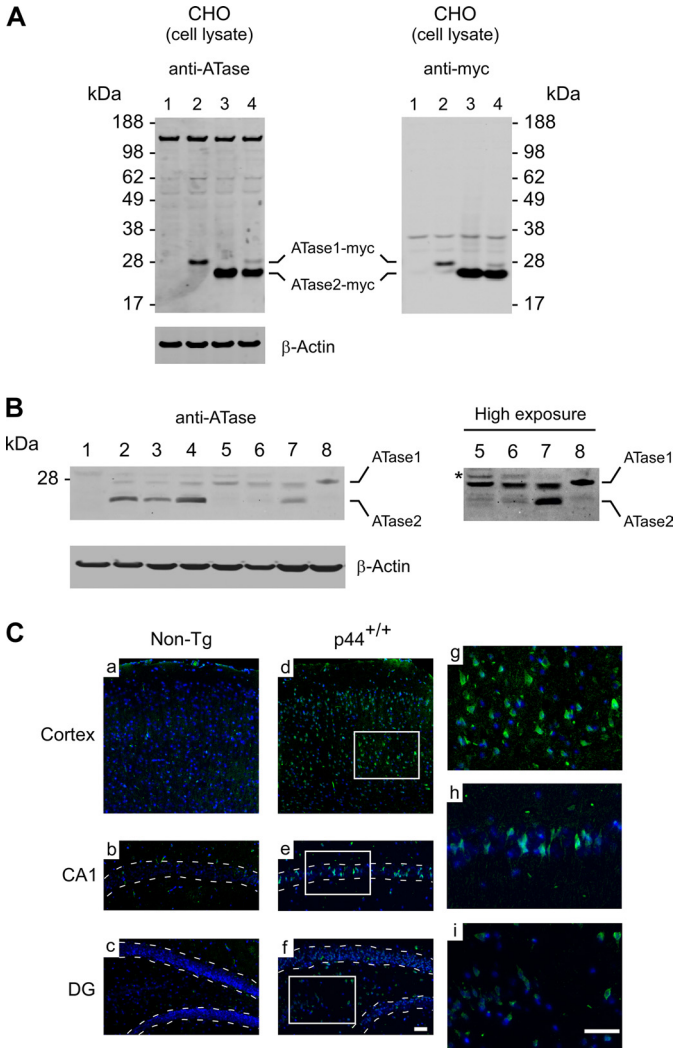

FIGURE 1. **ATase1 and ATase2 are expressed in neurons.** *A*, Western blot assessment of CHO cells overexpressing human ATase1 and/or ATase2. *Left panel*: anti-ATase1/ATase2 antibody; *right panel*: anti-Myc antibody. *Lane 1*, control (non transfected) cells; *lane 2*, stable overexpression of ATase1; *lane 3*, stable overexpression of ATase2; *lane 4*, stable overexpression of both ATase1 and ATase2. *B*, Western blot showing the endogenous levels of ATase1 and ATase2 in different cellular systems. The *right panel* shows higher exposure of the same image. *Lane 1*, CHO cells; *lane 2*, H4 cells; *lane 3*, SH-SY5Y cells; *lane 4*, SHEP cells; *lane 5*, PC-12 cells; *lane 6*, mouse primary neurons (day 3 in culture); *lane 7*, mouse primary neurons (day 18 in culture); *lane 8*; whole mouse brain extract (cortex). *Asterisks* (*) indicates a background band that migrates immediately above the 28-kDa marker. *C*, ATase1/ATase2 immunolabeling in different brain areas of control/non-transgenic (*Non-Tg*) and $p44^{+/+}$ transgenic ($p44^{+/+}$) mice. *Panels g*, *h*, and *i* correspond to higher magnification images of the areas indicated in *d*, *e*, and *f*, respectively. *Cortex*, frontal cortex; *CA1*, cornu ammonis (area 1), *DG*, dentate gyrus. Bar in *f*, 50 μm; bar in *i*, 50 μm.

RESULTS AND DISCUSSION

ATase1 and ATase2 Are Expressed in Neurons and Are Up-regulated in AD Brains—To confirm the relevance of ATase1 and ATase2 for AD neuropathology, we first assessed whether they are expressed in the brain and in cellular systems that are relevant for the study of the nervous system. Fig. 1*A* shows that the commercially available antibody used in this study could recognize transgenic ATase1 and ATase2 in Chinese Hamster Ovary (CHO) cells overexpressing Myc-tagged versions of the human proteins. Neither acetyltransferase could be signifi-

cantly detected in non-transfected CHO cells. We next assessed the expression levels of the endogenous acetyltransferases in human neuroglioma (H4), human neuroblastoma (SH-SY5Y and SHEP) and rat pheochromocytoma (PC-12) cells as well as mouse primary neurons and mouse cerebral cortex. Both ATase1 and ATase2 were identified, albeit with different intensity (Fig. 1*B*). Specifically, ATase1 appeared to be equally expressed while ATase2 appeared to be more predominant in H4, SH-SY5Y and SHEP cells. Detection of ATase2 in PC-12 cells required longer exposure (Fig. 1*B*; *right panel*). Assessment of a total extract of mouse cerebral cortex showed significant expression of ATase1 but low expression of ATase2 (Fig. 1*B*; *lane 8*). However, both were detectable in mouse primary neurons (Fig. 1*B*). The profile of ATase2 expression in primary neurons and total brain lysates seems to suggest preferential expression in neurons (see also later).

The expression levels of ATase2 increased with the age of the primary neurons (Fig. 1*B*; compare *lanes 6* and *7*). Both we and other groups have shown that, when in culture, primary neurons display an internal timing that mimics cellular senescence (16, 20). In particular, we reported that the levels of endogenous ceramide increase with the age of the culture (16). We also reported that ceramide treatment increases the mRNA levels of both ATase1 and ATase2 (14). Therefore, the activation of ATase2 in "older" neurons is consistent with our previous findings. We also noticed that ATase2 is more tightly regulated by ceramide than ATase1 (supplemental Fig. S1). Therefore, the above results indicate that both acetyltransferases are expressed in the brain and neurons as well as in cell lines that are commonly used for the study of the nervous system. They also suggest that in contrast to ATase1, which is constitutively expressed, ATase2 might act as a regulated form of acetylCoA:lysine acetyltransferase.

Histological assessment of ATase1 and ATase2 expression in non-transgenic (Non-Tg) and $p44^{+/+}$ transgenic ($p44^{+/+}$) mice showed a marked up-regulation in the latter as well as a preferential expression in neurons (Fig. 1*C*). $p44^{+/+}$ mice overexpress Δ40p53, a short isoform of the tumor suppressor and longevity assurance protein p53. As a result, they develop a progeroid phenotype that mimics an accelerated form of aging (21), which includes premature cognitive and synaptic deficits as well as an accelerated form of AD-like neuropathology (19). The up-regulation observed in $p44^{+/+}$ mice is consistent with the results obtained with "young" and "old" neurons (Fig. 1*B*, *lanes 6* and *7*). The histological assessment also revealed significant expression of the ATases in cortical neurons (Fig. 1*C*, *panels a*, *d*, and *g*) as well as in the pyramidal neurons of the *cornu ammonis* (CA) (Fig. 1*C*, *panels b*, *e*, and *h*). However, in the dentate gyrus, they appeared to be preferentially expressed in the polymorphic layer rather than in the granular cells of the stratum granulosum (Fig. 1*C*, *panels c*, *f*, and *i*). This was also observed in human tissue (Fig. 2*A*), perhaps indicating conserved functions of the ATases between mice and humans. The possible biological as well as pathological implications of this differential expression remain to be determined.

Histological assessment of AD brain tissue produced different outcomes. Increased labeling was consistently observed in the dentate gyrus, although mostly associated with non-neuronal cells, perhaps reflected by the gliosis that is known to occur in AD (Fig. 2*B*, *panels a*, *f*, *k* and *b*, *g*, *l*). Importantly, glial cells are also known to actively participate in the progression of AD neuropathology (22–25). No apparent change was observed in the CA areas (Fig. 2*B*, *panels c*, *h* and *m*). However, the CA was also characterized by neuronal loss, which affected our ability to compare levels of expression. Whether this is due to reduced viability of the neurons that overexpress the ATases remains to be assessed. Increased labeling was also observed throughout the frontal cortex, where it appeared to be almost exclusively associated with neuronal cells (Fig. 2*B*, *panels d*, *i*, *n* and *e*, *j*, *o*).

Direct assessment of ATase1 and ATase2 protein levels in the frontal cortex of late-onset AD patients revealed increased levels of ATase1 when compared with age-matched controls (Fig. 2*C*). Unfortunately, we were not able to detect ATase2, perhaps due to its preferential expression in neurons (see Fig. 1*B*). It is worth remembering that, although with great variations between different brain areas, neurons typically represent 2 to 15% of the total mass of the brain (26). This "low abundance" greatly limits our ability to assess the expression levels of proteins that are preferentially (or exclusively) expressed in neurons when using Western blot of total brain lysates. The preferential expression of ATase2 in neurons is consistent with the results displayed in Fig. 1*B*. In order to assess the levels of ATase2 and corroborate the above findings as well, we decided to use real-time quantitation of mRNA levels, which provides higher sensitivity. The results show increased levels of both transferases in AD brains (Fig. 2*D*), thus confirming the histological data.

ATase1 and ATase2 Inhibitors Down-regulate Both Levels and Activity of BACE1—We previously described a fluorescent assay that is able to assess the acetylCoA:lysine acetyltransferase activity of ATase1 and ATase2 *in vitro* (14). The assay employs affinity-purified ATase1 or ATase2 (as enzymes), acetyl-CoA (as donor of the acetyl group) and a recombinant peptide corresponding to the N-terminal tail of the histone protein H3 (as acceptor of the acetyl group). The H3 peptide was preferred to BACE1 because it is acetylated in a conformation independent manner (data not shown) and, therefore, more suitable for large screening approaches. To identify possible ATase1 and ATase2 inhibitors we used the assay to screen a single library of 14,400 compounds. The screen identified 186 compounds able to inhibit ATase1, ATase2 or both *in vitro*. Importantly, 93 compounds were unique to our screen suggesting unique properties. Each compound was then screened for cytotoxic properties by using multiplex cytotoxicity assays on a variety of cell lines. Of the above 186 compounds, only 30 did not cause significant cytotoxicity when used at 10 μM final concentration. A summary of the screen is shown in supplemental Fig. S2. The above 30 compounds were individually screened on human neuroglioma (H4) cells for their ability to reduce the levels of BACE1 and the generation of Aβ. Two compounds, #9 (6-chloro-5H-benzo[a]phenoxazin-5-one) and #19 (2-chloro-3-(2-ethoxyanilino)-1,4-dihydronaphthalene-1,4-dione), produced significant changes and were object of further study.

The compounds display very different chemical and structural features (Fig. 3*A*), which probably explain the different

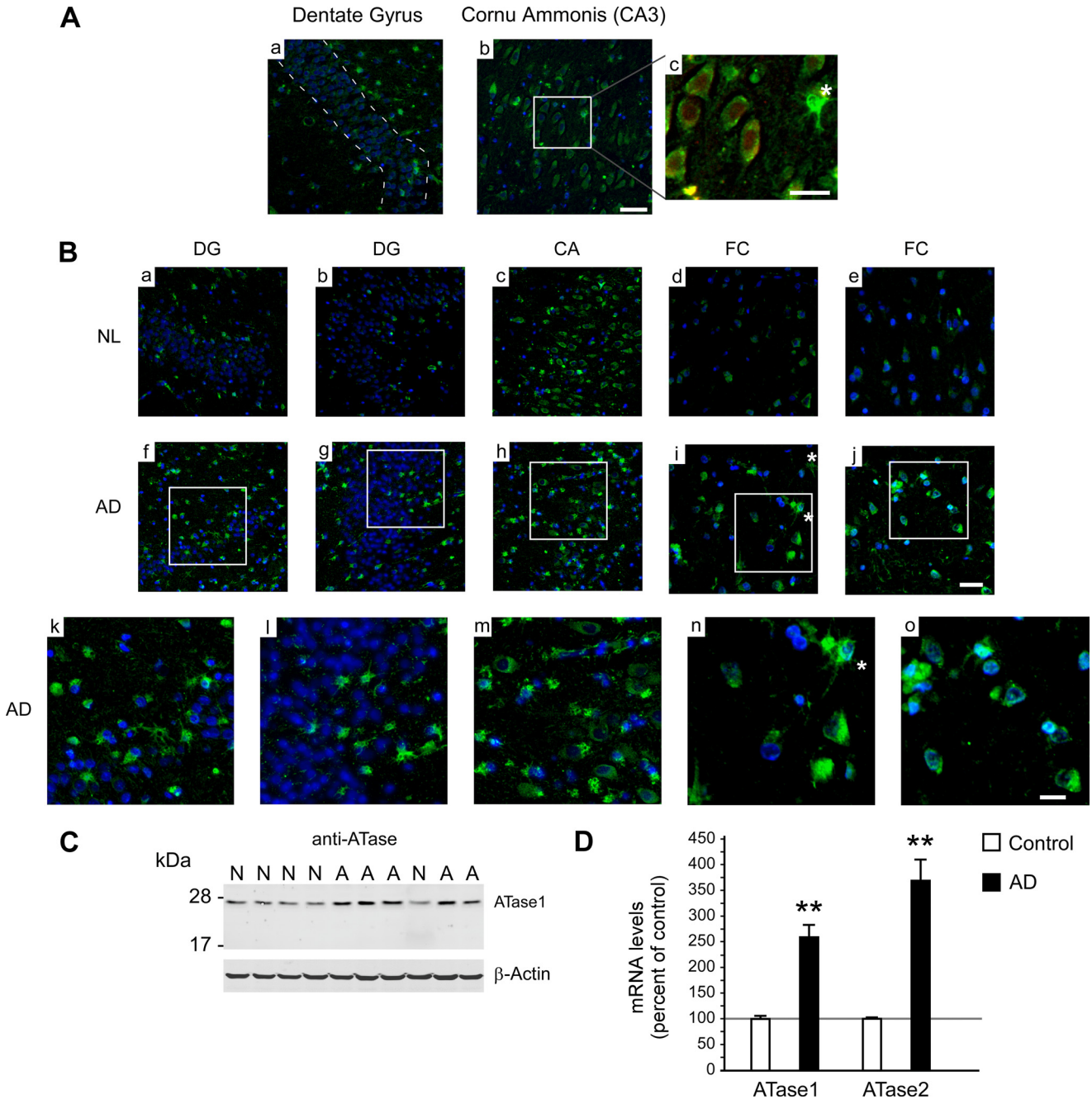

FIGURE 2. **ATase1 and ATase2 are up-regulated in the brain of AD patients.** *A*, ATase1/ATase2 immunolabeling in the dentate gyrus and cornu ammonis of control human brain. *Panel c* corresponds to a higher magnification image of the area indicated in *panel b*. Bar in *b*, 50 μm; bar in *c*, 25 μm. *Panel c* shows co-labeling of ATase1/ATase2 (*green*) and NeuN (neuronal marker; *red*). *Asterisk* (*) in *panel c* points to a single glial cell. *B*, ATase1/ATase2 immunolabeling in different brain areas of AD patients and age-matched controls (*NL*). *DG*, dentate gyrus; *CA*, cornu ammonis; *FC*, frontal cortex. *Panels k*, *l*, *m*, *n*, and *o* correspond to higher magnification images of the areas indicated in *f*, *g*, *h*, *i*, and *j*, respectively. Bar in *j*, 50 μm; bar in *o*, 25 μm. *Asterisks* (*) in *panels i* and *n* point to isolated glial cells. *C*, Western blot showing increased levels of ATase1 in the brain (frontal cortex) of AD patients. Lanes are labeled as *N* (for normal) and *A* (for AD). *D*, cDNA produced from the frontal cortex of late-onset AD patients ($n = 10$; average age: 70; age range: 60–91) and age-matched controls ($n = 10$; average age: 68; age range: 57–80) was analyzed by quantitative real-time PCR. Results were normalized against GAPDH levels and are expressed as percent of age-matched controls + S.E.; **, $p < 0.005$. Grading of AD patients is shown in supplemental Table S1.

kinetics of inhibition for acetyl-CoA, the donor of the acetyl group. In fact, compound 9 displayed a competitive inhibition with ATase1 and a non-competitive inhibition with ATase2, while compound 19 displayed non-competitive inhibition with both enzymes (Fig. 3, *B* and *C*). When tested *in vitro*, both compounds were able to inhibit the acetylation of affinity purified BACE1 (Fig. 4, *A* and *B*). To assess their biological effects, we treated human neuroglioma (H4) cells with 10 μM of each compound. In both cases, we observed a significant reduction in the levels of BACE1 (Fig. 4, *C–F*), although compound 9 appeared to act as a more potent inhibitor. This might be explained by different cell-permeability properties. In fact, the cLog *P* for compound 9 and 19 is 5.03 and 3.19, respectively. The cLog *P* (or partition coefficient) is an indication of partition properties of a compound between hydrophobic and hydrophilic compartments. Higher values indicate preferential distri-

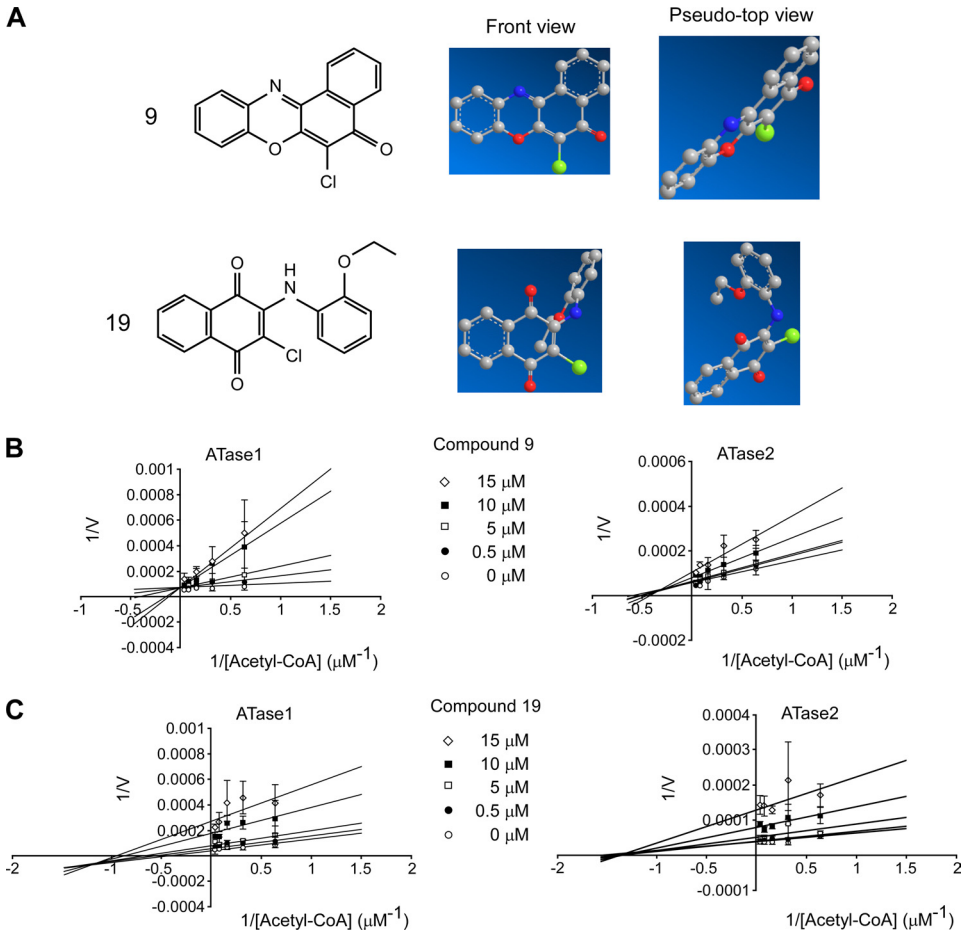

FIGURE 3. **Inhibition kinetics of compound 9 and 19.** *A*, schematic representation of the chemical and structural features of compound 9 and 19. *B* and *C*, Lineweaver-Burke plots for compound 9 (*B*) and 19 (*C*). Results are the mean of at least six independent determinations ± S.D.

bution in hydrophobic environments and, as such, increased permeability across biological membranes.

Interestingly, both compounds preferentially affected the mature form of BACE1 (Fig. 4, *C* and *E*). We previously reported that the ER-based acetylation of nascent BACE1 prevalently affects the levels of mature BACE1 (13, 14). In fact, non-acetylated mutants of BACE1 are correctly synthesized in the ER but rapidly degraded in the ERGIC before they can complete maturation (13, 15). The decreased levels of BACE1 were paralleled by decreased levels of Aβ in the conditioned media (Fig. 5*A*) and decreased cellular levels of C99 (Fig. 5*B*). As mentioned above, C99 is the immediate product of BACE1-mediated cleavage of APP, whereas Aβ represents one of the final products of the sequential processing of APP by BACE1 and γ-secretase (1). Parallel changes in C99 and Aβ directly reflect the steady-state levels and activity of BACE1. This was further confirmed by the decreased levels of the N-terminal product of APP (βsAPP), which is secreted as a result of BACE1-mediated cleavage (Fig. 5*C*). Interestingly, the reduced levels of βsAPP were paralleled by increased levels of αsAPP (Fig. 5*C*) perhaps as a compensatory effect caused by the down-regulation of BACE1 itself. αsAPP is generated by the α cleavage of APP and is not amyloidogenic.

Taken together, the above results indicate that both compound 9 and 19 affect the metabolism of BACE1 and the rate of Aβ generation. Finally, a similar decrease in BACE1 levels was also observed in SHEP (human neuroblastoma) cells indicating that the inhibitory properties of compound 9 and 19 were not limited to H4 cells (supplemental Fig. S3). However, H4 cells were preferentially used throughout this study because they allow a better separation of the mature and immature forms of BACE1 (compare Fig. 4 with supplemental Fig. S3).

N^{ϵ}-lysine acetylation was initially discovered as a covalent modification of nuclear and cytosolic proteins, which included histones, different families of transcription factors and cytoskeleton-associated proteins (27). Therefore, it is possible that, although screened for their ability to inhibit ATase1 and ATase2 *in vitro*, compound 9 and 19 might interfere with the acetylation of several other classes of proteins. To address this point we decided to assess the acetylation profile of both cytosolic and nuclear proteins. Neither compound 9 nor compound 19 produced significant changes (Fig. 6, *A* and *B*). The only consistent effect that we could observe was a slight reduction in the acetylation profile of the histone protein H4 (Fig. 6*C*) suggesting that compound 9 and compound 19 are highly selective. It is also worth stressing that neither compound inhibited the *in vitro* activity of the histone acetyltransferase p300/CBP (data not shown).

Next we decided to analyze structure-activity properties of both compounds by designing different chemical derivatives and assessing IC_{50s} *in vitro*. The results displayed in

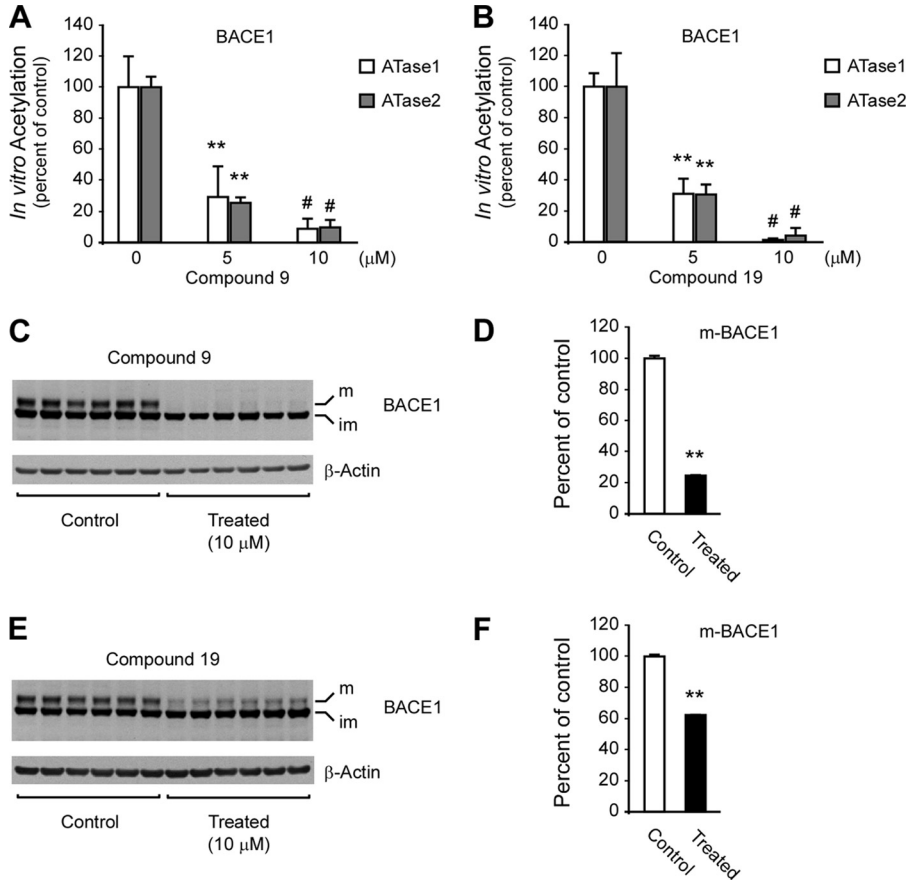

FIGURE 4. **Compounds 9 and 19 decrease the endogenous levels of BACE1.** *A* and *B*, affinity-purified ATases and BACE1 were co-incubated in the presence of [^{3}H]Acetyl-CoA and increasing concentrations of compound 9 (*A*) or 19 (*B*). For the determination of [^{3}H] incorporation, BACE1 was purified prior to scintillation liquid counting. The transfer activity of ATase1 and ATase2 in the absence of inhibitors was 3.05 ± 0.2 and 4.48 ± 0.3 nmol/h/mg of enzyme, respectively. Results are the mean ($n = 3$) + S.D.; **, $p < 0.005$; #, $p < 0.0005$. *C–F*, H4 cells were treated with either compound 9 or 19 for 48 h prior to Western blot assessment of BACE1 levels in total cell lysates (*C–F*). Representative Western blots are shown in *C* and *E* while respective quantifications are shown in *D* and *F*. Both mature (*m*) and immature (*im*) BACE1 are shown.

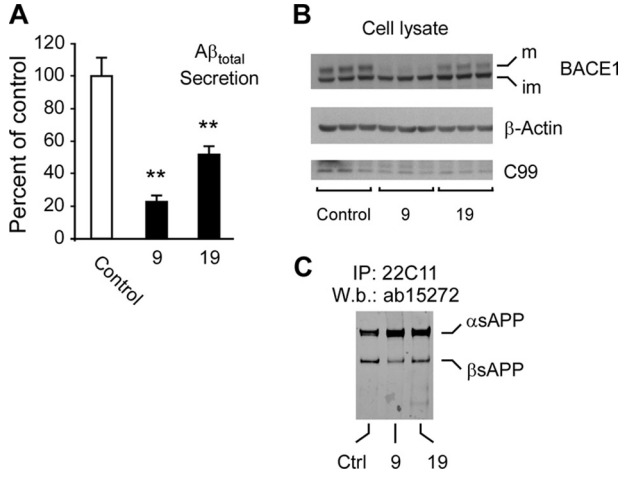

FIGURE 5. **Compounds 9 and 19 decrease levels and activity of BACE1.** H4 cells were treated with either compound 9 or 19 for 48 h prior to ELISA determination of secreted Aβ (*A*), and Western blot assessment of C99 (*B*) and αsAPP/βsAPP levels (*C*). C99 and βsAPP are the immediate products of BACE1-mediated cleavage of APP while αsAPP is the product of the α cleavage of APP. Both mature (*m*) and immature (*im*) BACE1 are shown. Aβ results are the mean ($n = 6$) + S.D.; **, $p < 0.005$.

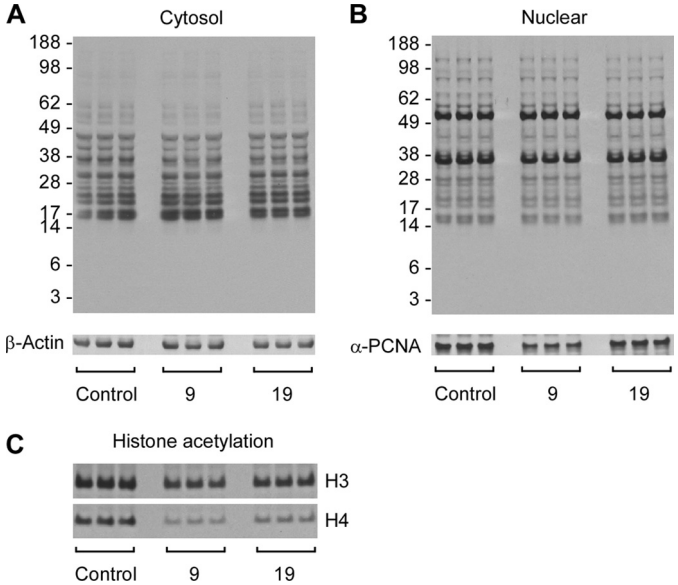

FIGURE 6. **Compounds 9 and 19 do not affect the lysine acetylation profile of cytosolic or nuclear proteins.** *A* and *B*, H4 cells were treated with either compound 9 or 19 for 48 h prior to Western blot assessment of the acetylation profile of cytosolic (*A*) and nuclear (*B*) proteins. *C*, The nuclear fraction used in (*B*) was also used to assess the lysine acetylation profile of the histone proteins H3 and H4. α-PCNA (*B*) also serves as loading control for *C*.

supplemental Tables SII-SIII and supplemental Figs. S4–S8 show that some modifications improved while others abolished the inhibitory properties of the parent compound. Although

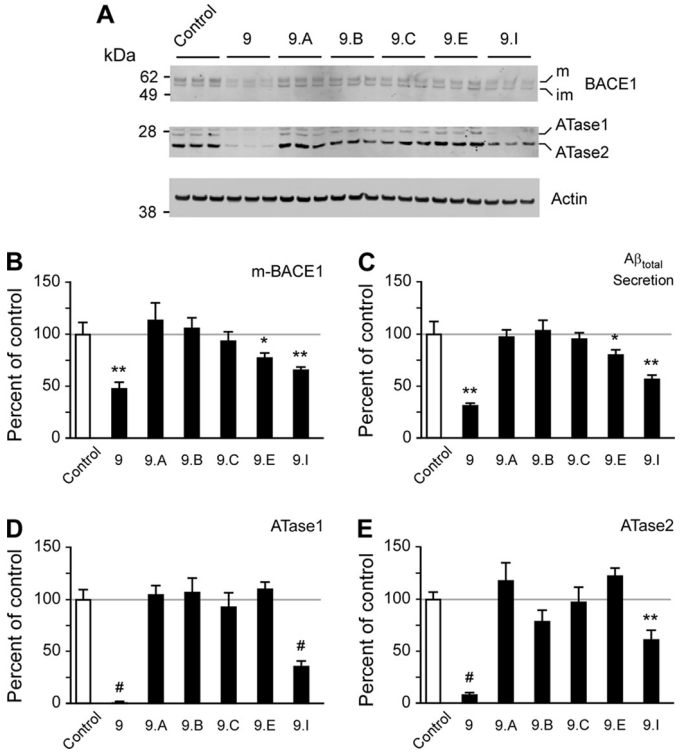

FIGURE 7. **Effect of compound 9 and derivatives on ATase1 and ATase2 levels.** *A*, H4 cells were treated with the indicated compounds (10 μM) for 48 h prior to Western blot assessment of BACE1 and ATase1/ATase2 levels in total cell lysates. *B*, *D*, and *E*, quantification of changes are expressed as percent of control (vehicle) and are the mean ($n = 3$) + S.D.; *, $p < 0.05$; **, $p < 0.005$; #, $p < 0.0005$. *C*, ELISA determination of secreted Aβ in the conditioned media of the experiment described in *A*. Results are expressed as percent of control (vehicle) and are the mean ($n = 3$) + S.D.; *, $p < 0.05$; **, $p < 0.005$.

the trend was overall similar, we observed some degree of difference when comparing IC_{50s} for ATase1 and ATase2, suggesting that certain structural determinants affect the two enzymes differently. Overall, the results described in supplemental Tables SII-SIII and supplemental Figs. S4–S8 indicate that the inhibitory properties of both compound 9 and 19 are tightly structure-dependent. This conclusion probably explains the high degree of selectivity that we observed in cellular systems.

Compound 9 Causes Apparent Molecular Instability and Degradation of ATase1 and ATase2—To assess whether the chemical modifications introduced in compound 9 also affected the biological properties, we tested the most active derivatives in cellular systems. H4 cells were treated with 10 μM of compound 9, 9.A, 9.B, 9.C, 9.E, and 9.I. The results show that only 9.I retained significant ability to affect the levels of BACE1 (Fig. 7, *A* and *B*) and the generation of Aβ (Fig. 7*C*). Surprisingly, these results appeared to correlate with the endogenous levels of ATase1 and ATase2. In fact, both compound 9 and 9.I were able to significantly down-regulate the expression of the acetyltransferases (Fig. 7). Compound 9, which was more active in down-regulating the ATases, also produced a more dramatic decrease in BACE1 levels (Fig. 7). The close relationship between levels of the ATases and BACE1 was dose dependent (Fig. 8, *A–D*). Because, the above experiments might potentially be affected by our ability to detect endogenous ATase1 and ATase2, we also treated CHO cells over-expressing transgenic ATase1 or ATase2. Western blot assessment of ATase1 and ATase2 levels confirmed that compound 9 significantly decreases the levels of both proteins (Fig. 8*E*). This effect appeared to be more dramatic with ATase1 (Fig. 8*E*), perhaps

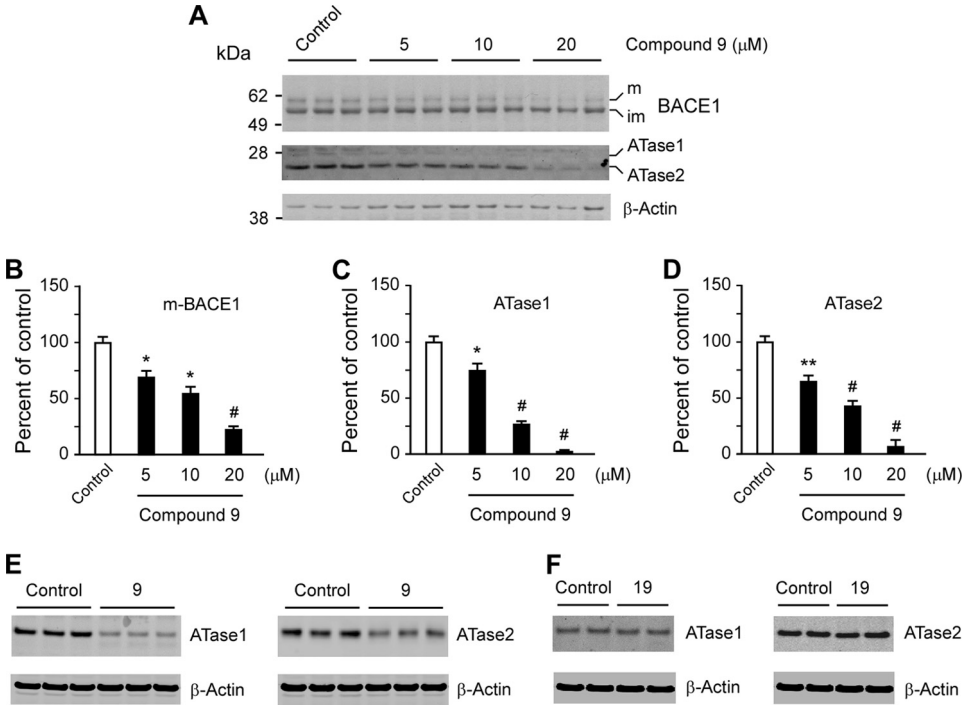

FIGURE 8. **Compound 9 causes the degradation of ATase1 and ATase2.** *A–D*, H4 cells were treated with increasing concentrations of compound 9 for 48 h prior to Western blot assessment of BACE1 and ATase1/ATase2 levels in total cell lysates. *B–D*, quantification of changes are expressed as percent of control (vehicle) and are the mean ($n = 3$) + S.D.; *, $p < 0.05$; **, $p < 0.005$; #, $p < 0.0005$. Both mature (*m*) and immature (*im*) BACE1 are shown. *E* and *F*, CHO cells overexpressing either ATase1 or ATase2 were treated with 10 μM compound 9 (*E*) or 19 (*F*) for 48 h prior to Western blot assessment of ATase1 and ATase2 levels in total cell lysates.

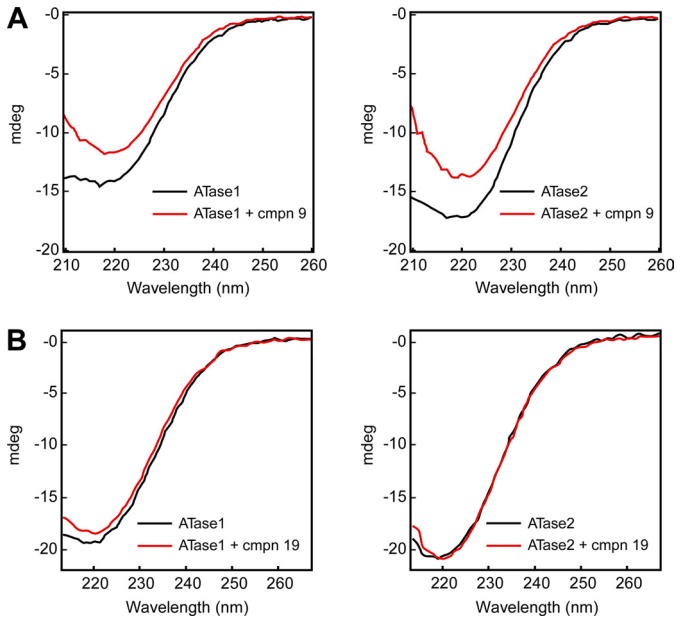

FIGURE 9. **Compound 9 causes conformational changes of ATase1 and ATase2.** *A* and *B*, circular dichroism spectra of affinity-purified ATase1 and ATase2 in the presence or absence of 10 μM compound 9 (*A*) or compound 19 (*B*).

explained by the competitive mechanism of the inhibition (see Fig. 3*B*). Finally, no effect was observed with compound 19 (Fig. 8*F*) suggesting that the ability to down-regulate the ATases is an intrinsic feature of compound 9.

Real-time determination of ATase1 and ATase2 mRNA levels following treatment with compound 9 did not reveal any difference (data not shown) suggesting that the down-regulation of the ATases occurs at the protein level, perhaps due to the ability of compound 9 to induce some sort of unstable intermediate form of the ATases. This possibility was confirmed with circular dichroism, which measures the difference in the absorbances of left- and right-handed circularly polarized light. In fact, compound 9 (but not compound 19) caused a rapid and dramatic change in both ellipticity and absorption of the purified ATases, reflecting structural changes in the helix/strand status of the ligand-bound protein (Fig. 9). Therefore, based on the above results, we can conclude that compound 9 causes conformational changes of the ATases (Fig. 9) that result in biochemical inhibition of their acetylCoA:lysine acetyltransferase activity (Fig. 3*B*) but also in the generation of unstable forms of the enzymes that are rapidly degraded (Fig. 8).

In conclusion, the results reported here confirm that both ATase1 and ATase2 regulate levels and activity of BACE1, and play an important role in AD neuropathology. The identification of specific inhibitors might help us further dissect the biochemistry as well as the biological relevance of both acetyltransferases. Finally, they might serve as a novel strategy to prevent AD dementia.

Acknowledgments—We thank Dr. James Malter for critical reading of an early version of this manuscript. The human brain tissue was provided by the Neuropathology Core of the Wisconsin ADRC established by NIH/NIA (P50-AG033514). We are grateful to Dr. Darrell R. McCaslin for help with circular dichroism.

REFERENCES

1. Puglielli, L. (2008) Aging of the brain, neurotrophin signaling, and Alzheimer disease: is IGF1-R the common culprit? *Neurobiol. Aging* **29,** 795–811
2. Lambert, M. P., Barlow, A. K., Chromy, B. A., Edwards, C., Freed, R., Liosatos, M., Morgan, T. E., Rozovsky, I., Trommer, B., Viola, K. L., Wals, P., Zhang, C., Finch, C. E., Krafft, G. A., and Klein, W. L. (1998) Diffusible, nonfibrillar ligands derived from Aβ1–42 are potent central nervous system neurotoxins. *Proc. Natl. Acad. Sci. U.S.A.* **95,** 6448–6453
3. Lansbury, P. T., Jr. (1999) Evolution of amyloid: what normal protein folding may tell us about fibrillogenesis and disease. *Proc. Natl. Acad. Sci. U.S.A.* **96,** 3342–3344
4. Klein, W. L., Krafft, G. A., and Finch, C. E. (2001) Targeting small Aβ oligomers: the solution to an Alzheimer disease conundrum? *Trends Neurosci.* **24,** 219–224
5. Haass, C., and Steiner, H. (2001) Protofibrils, the unifying toxic molecule of neurodegenerative disorders? *Nat. Neurosci.* **4,** 859–860
6. Cleary, J. P., Walsh, D. M., Hofmeister, J. J., Shankar, G. M., Kuskowski, M. A., Selkoe, D. J., and Ashe, K. H. (2005) Natural oligomers of the amyloid-β protein specifically disrupt cognitive function. *Nat. Neurosci.* **8,** 79–84
7. Puzzo, D., Privitera, L., Leznik, E., Fà, M., Staniszewski, A., Palmeri, A., and Arancio, O. (2008) Picomolar amyloid-β positively modulates synaptic plasticity and memory in hippocampus. *J. Neurosci.* **28,** 14537–14545
8. Giliberto, L., Zhou, D., Weldon, R., Tamagno, E., De Luca, P., Tabaton, M., and D'Adamio, L. (2008) Evidence that the Amyloid β Precursor Protein-intracellular domain lowers the stress threshold of neurons and has a "regulated" transcriptional role. *Mol. Neurodegener.* **3,** 12
9. Ghosal, K., Vogt, D. L., Liang, M., Shen, Y., Lamb, B. T., and Pimplikar, S. W. (2009) Alzheimer disease-like pathological features in transgenic mice expressing the APP intracellular domain. *Proc. Natl. Acad. Sci. U.S.A.* **106,** 18367–18372
10. Cai, H., Wang, Y., McCarthy, D., Wen, H., Borchelt, D. R., Price, D. L., and Wong, P. C. (2001) BACE1 is the major β-secretase for generation of Aβ peptides by neurons. *Nat. Neurosci.* **4,** 233–234
11. Luo, Y., Bolon, B., Kahn, S., Bennett, B. D., Babu-Khan, S., Denis, P., Fan, W., Kha, H., Zhang, J., Gong, Y., Martin, L., Louis, J. C., Yan, Q., Richards, W. G., Citron, M., and Vassar, R. (2001) Mice deficient in BACE1, the Alzheimer β-secretase, have normal phenotype and abolished β-amyloid generation. *Nat. Neurosci.* **4,** 231–232
12. Gravitz, L. (2011) Drugs: a tangled web of targets. *Nature* **475,** S9–11
13. Costantini, C., Ko, M. H., Jonas, M. C., and Puglielli, L. (2007) A reversible form of lysine acetylation in the ER and Golgi lumen controls the molecular stabilization of BACE1. *Biochem. J.* **407,** 383–395
14. Ko, M. H., and Puglielli, L. (2009) Two endoplasmic reticulum (ER)/ER Golgi intermediate compartment-based lysine acetyltransferases post-translationally regulate BACE1 levels. *J. Biol. Chem.* **284,** 2482–2492
15. Jonas, M. C., Costantini, C., and Puglielli, L. (2008) PCSK9 is required for the disposal of non-acetylated intermediates of the nascent membrane protein BACE1. *EMBO Rep.* **9,** 916–922
16. Costantini, C., Scrable, H., and Puglielli, L. (2006) An aging pathway controls the TrkA to p75NTR receptor switch and amyloid β-peptide generation. *EMBO J.* **25,** 1997–2006
17. Ko, M. H., and Puglielli, L. (2007) The sterol carrier protein SCP-x/pro-SCP-2 gene has transcriptional activity and regulates the Alzheimer disease γ-secretase. *J. Biol. Chem.* **282,** 19742–19752
18. Jonas, M. C., Pehar, M., and Puglielli, L. (2010) AT-1 is the ER membrane acetyl-CoA transporter and is essential for cell viability. *J. Cell Sci.* **123,** 3378–3388
19. Pehar, M., O'Riordan, K. J., Burns-Cusato, M., Andrzejewski, M. E., del Alcazar, C. G., Burger, C., Scrable, H., and Puglielli, L. (2010) Altered longevity-assurance activity of p53:p44 in the mouse causes memory loss, neurodegeneration and premature death. *Aging Cell* **9,** 174–190
20. Shen, Q., Wang, Y., Dimos, J. T., Fasano, C. A., Phoenix, T. N., Lemischka, I. R., Ivanova, N. B., Stifani, S., Morrisey, E. E., and Temple, S. (2006) The timing of cortical neurogenesis is encoded within lineages of individual progenitor cells. *Nat. Neurosci.* **9,** 743–751

21. Maier, B., Gluba, W., Bernier, B., Turner, T., Mohammad, K., Guise, T., Sutherland, A., Thorner, M., and Scrable, H. (2004) Modulation of mammalian life span by the short isoform of p53. *Genes Dev.* **18,** 306–319
22. Ilieva, H., Polymenidou, M., and Cleveland, D. W. (2009) Non-cell autonomous toxicity in neurodegenerative disorders: ALS and beyond. *J. Cell Biol.* **187,** 761–772
23. Attwell, D., Buchan, A. M., Charpak, S., Lauritzen, M., Macvicar, B. A., and Newman, E. A. (2010) Glial and neuronal control of brain blood flow. *Nature* **468,** 232–243
24. Perry, V. H., Nicoll, J. A., and Holmes, C. (2010) Microglia in neurodegenerative disease. *Nat. Rev. Neurol.* **6,** 193–201
25. Rodríguez, J. J., and Verkhratsky, A. (2011) Neuroglial roots of neurodegenerative diseases? *Mol. Neurobiol.* **43,** 87–96
26. Azevedo, F. A., Carvalho, L. R., Grinberg, L. T., Farfel, J. M., Ferretti, R. E., Leite, R. E., Jacob Filho, W., Lent, R., and Herculano-Houzel, S. (2009) Equal numbers of neuronal and nonneuronal cells make the human brain an isometrically scaled-up primate brain. *J. Comp. Neurol.* **513,** 532–541
27. Yang, X. J., and Seto, E. (2007) HATs and HDACs: from structure, function, and regulation to novel strategies for therapy and prevention. *Oncogene* **26,** 5310–5318